

Photorefractive effect in doped $\text{Pb}_5\text{Ge}_3\text{O}_{11}$ and in $(\text{Pb}_{1-x}\text{Ba}_x)_5\text{Ge}_3\text{O}_{11}$

Xuefeng Yue,^{a)} S. Mendricks, Yi Hu, H. Hesse, and D. Kip

Fachbereich Physik der Universität Osnabrück, Barbarastrasse 7 D-49069 Osnabrück, Germany

(Received 4 August 1997; accepted for publication 15 December 1997)

The photorefractive effect is studied in ferroelectric lead germanate crystals $\text{Pb}_5\text{Ge}_3\text{O}_{11}$, including undoped, Fe- and Rh-doped crystals, as well as $(\text{Pb}_{1-x}\text{Ba}_x)_5\text{Ge}_3\text{O}_{11}$ solid solutions. Two kinds of processes are involved in photorefractive interactions: a fast response with a time constant generally less than 1 s and the formation of slow gratings with time constants of several hours for intensities in the range of 1–30 kW/m². Basic photorefractive parameters corresponding to the fast response, such as dark- and photoconductivities, the sign of the main charges involved in the transport process, effective trap densities, and activation energies are determined. Compared to theoretical predictions the measured effects are too small which is attributed mainly to electron-hole competition. © 1998 American Institute of Physics. [S0021-8979(98)00407-1]

I. INTRODUCTION

Many oxide crystals exhibit a photorefractive effect, which means that inhomogeneous illumination leads to excitation and redistribution of charge carriers. Space-charge fields build up and modulate the refractive index via the electrooptic effect. Crystals with this property are of great interest for applications like optical data storage or signal processing.¹ The research on photorefractive materials has been concentrated both on crystals exhibiting very large effects² and on so-called nonideal materials.³ Improving or tailoring the properties of known materials as well as the search for new photorefractive crystals have gained much attention in recent years.

From our point of view a candidate for detailed investigations of the photorefractive effect is lead germanate $\text{Pb}_5\text{Ge}_3\text{O}_{11}$. Large single crystals were first grown by Iwasaki *et al.* in 1971.⁴ Lead germanate is ferroelectric below $T_C=178^\circ\text{C}$ and shows optical activity. Its linear electrooptic coefficients r_{13} and r_{33} are fairly large with values of 10.5 pm/V and 15.3 pm/V, respectively.⁵ But until now, only little is known about the photorefractive effect in this material. Most of the publications about lead germanate deal with electrooptic, pyro- and piezoelectric properties and with its optical activity. To our knowledge there is only one letter demonstrating the photorefractive effect in undoped lead germanate which was published in 1990 by Królikowsky *et al.*⁶ In many cases doping with transition-metal ions can greatly change physical parameters which are of relevance for the photorefractive effect. Furthermore, in lead germanate the adding of Ba has a strong influence on phase transition temperature and electric conductivity. Information concerning the effect on the photorefractive effect is also of importance for material research.

In the present contribution we report in detail on the photorefractive effect in undoped and doped lead germanate crystals as well as in $(\text{Pb}_{1-x}\text{Ba}_x)_5\text{Ge}_3\text{O}_{11}$ solid solutions. In section II the growth and preparation of the crystals are

briefly described, and the absorption spectra for various samples are presented. Then we explain in section III the experimental methods and theoretical considerations from which some basic photorefractive parameters can be obtained. Section IV contains detailed experimental results, including effective charge densities, dark- and photoconductivities, activation energies and electron-hole competition factors. Further discussions and remarks are presented in section V.

II. CRYSTAL GROWTH AND OPTICAL ABSORPTION

Lead germanate melts congruently and can be grown using standard Czochralski equipment. All crystals were grown in the crystal growth laboratory of the University of Osnabrück. Typical pulling and rotation rates are 1.4 mm/h and 30 rpm. All crystals were pulled along the *c* direction. Crystallization takes place at 738 °C in a structure belonging to the point group $\bar{6}$. At $T_c=178^\circ\text{C}$ lead germanate undergoes a second-order phase transition from the paraelectric to the ferroelectric phase with point group 3. After growth the crystals were cut and polished. Subsequently, the crystals were poled by cooling from a temperature slightly above T_c down to room temperature by applying an electric field of about 0.3 kV/cm. Afterwards piezoelectric and pyroelectric measurements were carried out to prove that the single domain state is achieved. $\text{Pb}_5\text{Ge}_3\text{O}_{11}$ (PGO) crystals doped with Fe and Rh (dopant concentrations are given in mol ppm related to the Ge content of the melt) and $(\text{Pb}_{1-x}\text{Ba}_x)_5\text{Ge}_3\text{O}_{11}$ (PBGO) solid solutions with $x=0.01, 0.02, \text{ and } 0.04$ (x in the melt) were grown and samples were prepared. We describe the samples used in our experiments in Table I.

Utilizing a CARY-17D spectrometer we measured the optical absorption for different lead germanate samples for extraordinarily [Fig. 1(a)] and ordinarily polarized light in the wavelength range of 400–800 nm. The absorption coefficients α are calculated by taking into account multiple reflections at the front and back sides of the crystal with the use of the refractive indices of $\text{Pb}_5\text{Ge}_3\text{O}_{11}$.⁷ The absorption coefficients of all samples except those doped with Fe are

^{a)}Electronic mail: xyuefeng@rz.uni-osnabrueck.de

TABLE I. Descriptions of our samples used in the experiments.

Number	Crystal and dopant	Dimensions [$a \times b \times c$ (mm ³)]
PGO	Pb ₅ Ge ₃ O ₁₁	2.40 × 6.20 × 5.5
PBGO:0.01	(Pb _{0.99} Ba _{0.01}) ₅ Ge ₃ O ₁₁	1.90 × 5.30 × 6.25
PBGO:0.02	(Pb _{0.98} Ba _{0.02}) ₅ Ge ₃ O ₁₁	2.60 × 4.10 × 4.40
PBGO:0.04	(Pb _{0.96} Ba _{0.04}) ₅ Ge ₃ O ₁₁	3.10 × 6.50 × 6.76
PGO:500 Fe	Pb ₅ Ge ₃ O ₁₁ : 500 ppm Fe	1.80 × 4.00 × 5.50
PGO:1000 Fe	Pb ₅ Ge ₃ O ₁₁ : 1000 ppm Fe	1.90 × 5.10 × 6.80
PGO:500 Rh	Pb ₅ Ge ₃ O ₁₁ : 500 ppm Rh	2.50 × 4.65 × 6.85

small for extraordinarily polarized light of an Ar⁺ laser (wavelength $\lambda = 514.5$ nm). The presence of Ba leads to a decrease of absorption in the short wavelength range, while doping with Rh has almost no influence on the absorption spectrum. Compared with other samples, the Fe-doped samples have much larger absorption coefficients in the short wavelength range for extraordinarily polarized light. All doped samples show an appreciable dichroism which depends both on the doping and on the wavelength region. The same dependence of dichroism on wavelength is found

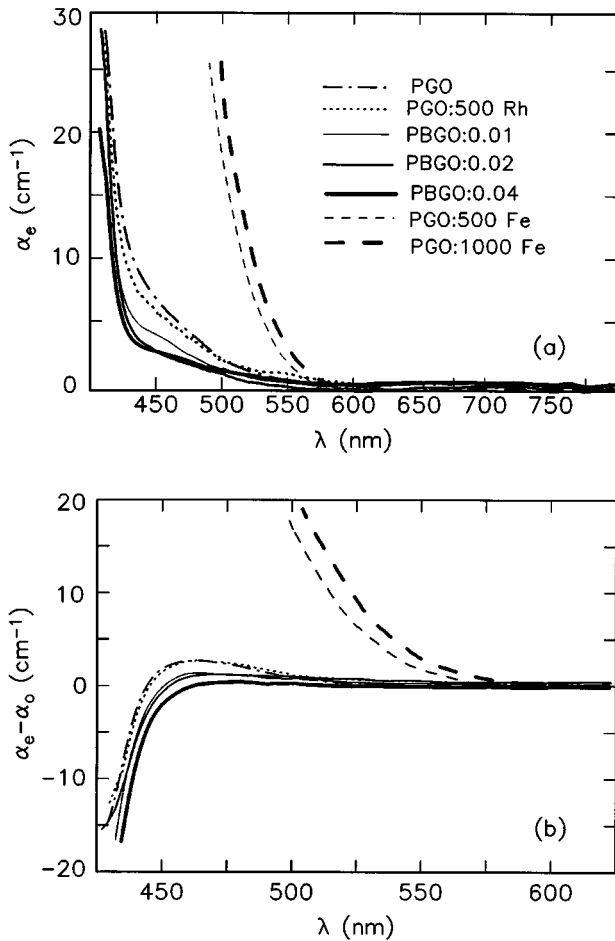


FIG. 1. Absorption spectra for lead germanate crystals with different dopings. (a) Absorption coefficient α_e for extraordinarily polarized light, and (b) difference ($\alpha_e - \alpha_o$) between the absorption coefficients for extraordinarily and ordinarily polarized light. The lines in (b) correspond to the legend used in (a).

in the undoped, Rh-doped and (Pb_{1-x}Ba_x)₅Ge₃O₁₁ solid solutions.

III. EXPERIMENTS AND THEORETICAL CONSIDERATIONS

A. Measurement of diffraction efficiency

A usual holographic experimental setup⁸ is used to measure the photorefractive properties of lead germanate crystals: Two expanded beams of an Ar⁺ laser ($\lambda = 514.5$ nm) of approximately the same intensity (intensity modulation $m > 0.98$) and with extraordinary polarization are utilized to write gratings with a grating vector parallel to the c axis of the crystals. The formation of gratings is monitored by a weak extraordinarily polarized He-Ne laser beam ($\lambda = 632.8$ nm) incident at the Bragg angle. If there is no specified description, the spatial frequency of the grating is $K = 2.35 \mu\text{m}^{-1}$ in holographic recording. A heatable crystal holder is used to stabilize the crystal temperature in the range from room temperature to 60 °C. Silver paste electrodes are put onto the two c faces of the samples so that a DC electric field can be applied to the crystals along the c axis.

The diffraction efficiency is defined as the ratio between diffracted beam intensity and total transmitted readout beam intensity without grating. It is derived from Kogelnik's formula:⁹

$$\eta = \sin^2(\pi \Delta n d / \lambda \cos \theta_r), \quad (1)$$

where Δn is the modulation of the refractive index, d is the thickness of the crystal, and θ_r is the Bragg angle between surface normal and readout beam inside the crystal. In photorefractive materials the refractive index modulation is determined by the electrooptic coefficient r_{eff} and the space-charge field E_{sc} :¹⁰

$$\Delta n = -\frac{1}{2} n^3 r_{\text{eff}} E_{\text{sc}}, \quad (2)$$

where n is the effective refractive index ($n = n_o n_e / \sqrt{n_e^2 \sin^2 \theta + n_o^2 \cos^2 \theta}$), θ is the half angle between the two interacting beams inside the crystal, and $n_{o,e}$ are the refractive indices for ordinarily and extraordinarily polarized light.

In a crystal of point group 3 and for the extraordinarily polarized writing beams, the effective electrooptic coefficient is

$$r_{\text{eff}} = \frac{1}{2n^4} \{ n_o^4 r_{22} \sin \beta (\cos 2\theta - \cos 2\beta) [n_o^4 r_{13} (\cos 2\theta - \cos 2\beta) + 4n_e^2 n_e^2 r_{51} \sin^2 \beta + n_e^4 r_{33} \sin \beta (\cos 2\theta + \cos 2\beta)] \cos \beta \}, \quad (3)$$

where β is the angle between the grating vector and the c axis measured inside the crystal. If the grating vector is directed along the c axis of the crystal and ignoring the small difference of refractive indices n and $n_{o,e}$, the effective electrooptic coefficient is simplified to

$$r_{\text{eff}} = -r_{13} \sin^2 \theta + r_{33} \cos^2 \theta. \quad (4)$$

For ordinarily polarized light and the symmetric condition ($\beta=0$) the effective electrooptic coefficient is r_{13} , which is slightly smaller than that for extraordinarily polarized light.

The space-charge field caused by a sinusoidal intensity pattern with modulation $m \sim 1$ is given by

$$E_{sc} = CE_Q \left(\frac{E_0^2 + E_D^2}{E_0^2 + (E_D + E_Q)^2} \right)^{1/2}, \quad (5)$$

where E_0 is the applied electric field, and E_D and E_Q are the diffusion and the limiting space-charge field, respectively:

$$E_D = Kk_B T/e, \quad E_Q = eN_{eff}/K\epsilon\epsilon_0. \quad (6)$$

Here k_B is the Boltzmann constant, T is the temperature, ϵ_0 the permittivity of free space, and ϵ is the dielectric constant. C is a factor which reduces the space-charge field due to the following reasons:

(1) *Dark conductivity*—If the dark conductivity σ_d is not negligible compared to the photo conductivity σ_p , the space-charge field is reduced by a factor χ which can be expressed as

$$\chi = \frac{1}{1 + \sigma_d/\sigma_p}. \quad (7)$$

(2) *Electron-hole competition constant* $\xi(K)$ —The constant is less than unity if both the electrons and holes are involved in the charge transport process. The single-species electron-hole transport model predicts that the constant $\xi(K)$ is in the form of

$$\xi(K) = (\sigma_e - \sigma_h)/(\sigma_e + \sigma_h) \quad (8)$$

for small spatial frequency of the gratings.¹¹ Here $\sigma_{e,h}$ are electron and hole conductivity, respectively.

In addition, a correction constant has to be introduced to account for a reduction of the measured diffraction efficiency by different experimental parameters, such as multiple beam reflections, angular deviations of the readout beam from the Bragg angle,¹² and screening charge effects,¹³ if we apply an external electric field during the holographic recording.

The decay properties of the gratings can be monitored by a weak He-Ne laser beam during erasure. The inverse decay time constant τ^{-1} of the grating is described by

$$\tau^{-1} = (\sigma_d + \sigma_p)/\epsilon\epsilon_0, \quad (9)$$

with

$$\sigma_p \propto I^x. \quad (10)$$

A relation $x \leq 1$ is predicted by either a one-center model with changing concentrations of traps, a two-center model or a three-valence model.¹⁴ The intensity dependence of the inverse decay time constant is used to determine dark- and photoconductivity as well as the sublinearity of photoconductivity on intensity. Furthermore, the dark decay time constant τ_d has a temperature dependence given by

$$\tau_d = \tau_0 \exp(E_A/k_B T), \quad (11)$$

where τ_0 is the decay time constant when all the charges are thermally activated, and E_A is the activation energy. The temperature dependence of τ_d can be used to determine the activation energy E_A .

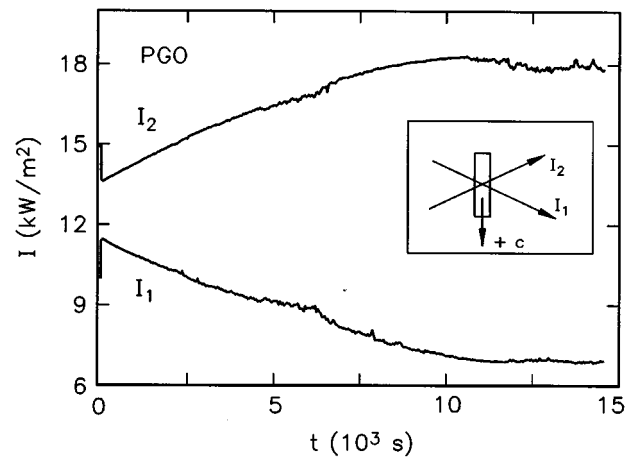


FIG. 2. An example of beam coupling in the undoped PGO sample with the orientation of the crystal shown in the inset. $I_{1,2}$ are transmitted intensities of two interacting beams. The grating spatial frequency is $K = 8.35 \mu\text{m}^{-1}$.

B. Measurement of beam-coupling gain

In two-wave mixing experiments, two extraordinarily polarized Ar^+ laser beams ($\lambda = 514.5 \text{ nm}$) are utilized. No external electric field is applied. Both transmitted beams are monitored and the exponential gain Γ is defined by

$$\Gamma = \frac{1}{d} \ln \left(\frac{I'_1 I_2}{I_1 I'_2} \right), \quad (12)$$

where $I'_{1,2}$ and $I_{1,2}$ are the transmitted intensities with and without coupling.

The relation between the exponential gain Γ and the beam crossing angle can be described by¹⁵

$$\Gamma = \frac{A \sin \theta_{ex}}{1 + B^{-2} \sin^2 \theta_{ex}} \frac{\cos 2\theta}{\cos \theta}, \quad (13)$$

where θ_{ex} is the half external beam crossing angle. The parameters A and B are connected with different crystal properties following the equations

$$A = Cr_{eff} \frac{8\pi^2 n^3 k_B T}{e\lambda^2}, \quad (14)$$

and

$$B = \frac{e\lambda}{4\pi} \left(\frac{N_{eff}}{\epsilon\epsilon_0 k_B T} \right)^{1/2}. \quad (15)$$

Both the effective charge density N_{eff} and the electron-hole competition factor $\xi(K)$ can be determined from the angular dependence of Γ . Furthermore, from the energy transfer direction the sign of the main charges involved in the charge transport can be deduced.

IV. EXPERIMENTAL RESULTS

A. Observation of multiple gratings

As an example of beam coupling we show a longtime recording of intensity variation during two-wave mixing in the undoped PGO sample in Fig. 2. The transmitted beam

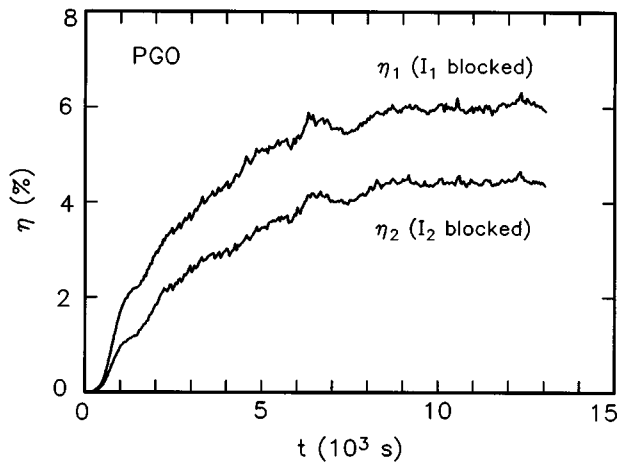


FIG. 3. Diffraction efficiency η measured by alternately using one of the writing beams as a readout beam during beam coupling. The optical orientation is the same as in Fig. 2.

intensities of $I_1 = 10 \text{ kW/m}^2$ and $I_2 = 15 \text{ kW/m}^2$ without grating are measured. After both beams are turned on, there is a fast energy exchange between them with a response time of less than 1 s. After several hundreds of seconds a slow grating appears gradually which causes an energy transfer towards the negative c direction, and in the final state the total energy exchange is in the negative c direction, too. We have determined the exponential gain corresponding to the fast grating to be $\Gamma_f = 0.98 \text{ cm}^{-1}$ and for the slow grating we find $\Gamma_s = 3.38 \text{ cm}^{-1}$. The grating spatial frequency is $K = 8.35 \mu\text{m}^{-1}$. Based on this observation we can exclude that the slow grating is formed only through a compensating process due to thermally excited charges. Both gratings have a non-zero phase shift with respect to the light pattern, and this is a characteristic property of the electrooptic photorefractive effect.

To check if there is an extinction grating involved in the slow process, we measure the diffraction efficiency by alternately reading the gratings during recording with one of the two writing beams. A computer controlled program measures the diffraction efficiency 1 s after the action of an electrical shutter. Thus only the slow grating is monitored because the fast grating decays completely in this time interval. The orientation of the sample with respect to the beams is shown in the inset of Fig. 2. We define η_1 and η_2 as the diffraction efficiencies probed by I_2 (I_1 is blocked) and I_1 (I_2 is blocked), respectively. Their dependences on interacting time are presented in Fig. 3. There is an obvious difference between η_1 and η_2 which indicates the presence of both a refractive index and an extinction grating shifted relative to each other.¹⁶

The slow grating with relatively large efficiency might be interesting for optical data storage, but in the present work we observe it only in the undoped PGO sample. The fast grating, however, can be written in all of the samples and the measurements show good reproducible results. In the following we concentrate mainly on fast grating which is of interest for real-time holography and information processing.

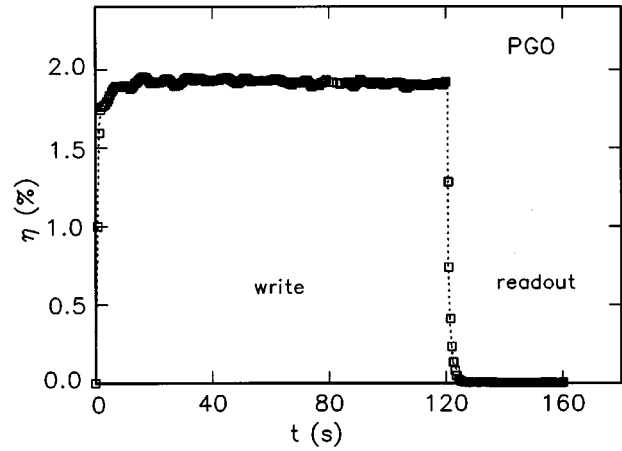


FIG. 4. Evolution of diffraction efficiency η during holographic recording and readout with an applied electrical field $E_0 = 10 \text{ kV/cm}$ in the undoped PGO sample. The wavelength and intensity of the writing beams are $\lambda = 514.5 \text{ nm}$ and $I = 5 \text{ kW/m}^2$. During the whole process the diffraction efficiency is probed by a weak He-Ne laser beam ($\lambda = 632.8 \text{ nm}$).

B. Fast grating

A typical time evolution of diffraction efficiency during holographic recording and decay in the undoped PGO sample is shown in Fig. 4, from which we see that in a time range of several minutes, only the fast grating is of importance. With an applied electric field of $E_0 = 10 \text{ kV/cm}$ and for a grating spatial frequency $K = 2.35 \mu\text{m}^{-1}$, the maximum diffraction efficiency is about 2% corresponding to a refractive index modulation of $\Delta n = 1.2 \times 10^{-5}$. After the writing beams are turned off, the grating decays quickly too. We observe a small response time constant of several hundred ms. To estimate the photorefractive recording sensitivity, we choose the definition given in Ref. 17 i.e., $S = \eta^{1/2}/W_0$, where η is the diffraction efficiency and W_0 the incident energy density. Then the sensitivity is determined as $S \sim 0.5 \text{ cm}^2/\text{J}$ which is about the same order as that of highly doped and lightly reduced LiNbO_3 .¹⁷ As has been already described in section IV A, there is an asymmetric energy transfer corresponding to the fast grating. The exponential gain depends on the polarization of the two interacting beams: Without electric field, the ratio of exponential gains for extraordinarily and ordinarily polarized beams is $\Gamma_e/\Gamma_o \approx 1.4$, which is in good agreement with the ratio of effective electrooptic coefficients corresponding to these two configurations.

1. Effective charge density N_{eff} and sign of charges

The dependence of refractive index modulation on the external electric field for different samples was measured and the results are presented in Fig. 5. The lines are theoretical fittings based on Eqs. (2)–(6) in section III A and the values of effective charge densities N_{eff} obtained are listed in Table II. It can be seen that the doping does not lead to an increase of the effective charge density. The larger the concentration of Ba, the smaller the effective charge density N_{eff} . Doping

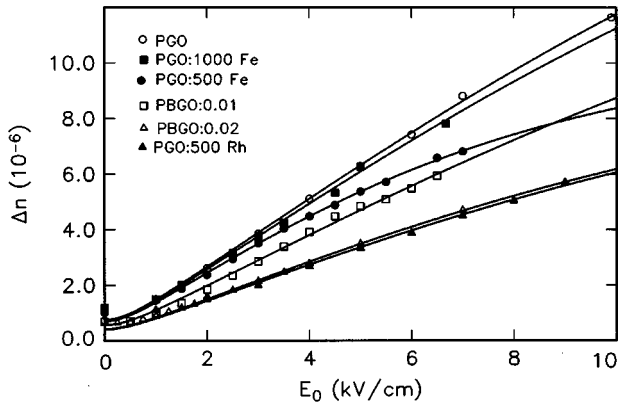


FIG. 5. Modulation of refractive index Δn as a function of applied electric field E_0 during holographic recording for different samples.

with Fe leads to an increase of N_{eff} . In both cases, however, the values of N_{eff} are smaller for the doped samples compared with the undoped sample.

The exponential gain in two-wave mixing was measured as a function of beam crossing angle for the undoped PGO sample. The value of N_{eff} determined in this measurement is $N_{\text{eff}} = 1.21 \times 10^{22} \text{ m}^{-3}$ which is in agreement with the result $N_{\text{eff}} = 1.16 \times 10^{22} \text{ m}^{-3}$ obtained by diffraction measurements. We estimate the error limits in all of our experiments to be about $\pm 10\%$.

Without external electric field and at the beginning of holographic recording the energy is always transferred towards the positive c direction in all of the samples used in our investigations. To determine the sign of the charges involved in the fast grating formation, one has to know the sign of the effective electrooptic coefficient r_{eff} . In our experiment, the θ is 2.6° (corresponding to $K = 2.35 \mu\text{m}^{-1}$). This corresponds to a positive effective electrooptic coefficient ($r_{\text{eff}} = 15.2 \text{ pm/V}$). From Eq. (4) we then conclude that the main charges involved in the charge transport responsible for the fast grating are holes.

2. Dark- and photoconductivity

The inverse decay time constants τ^{-1} of the photorefractive gratings are measured as a function of erase beam intensity I at room temperature for different samples as shown in Fig. 6. The lines are fittings to the experimental results using Eqs. (9) and (10). The parameters σ_d and x are listed again in Table II. In general doping reduces both the dark- and pho-

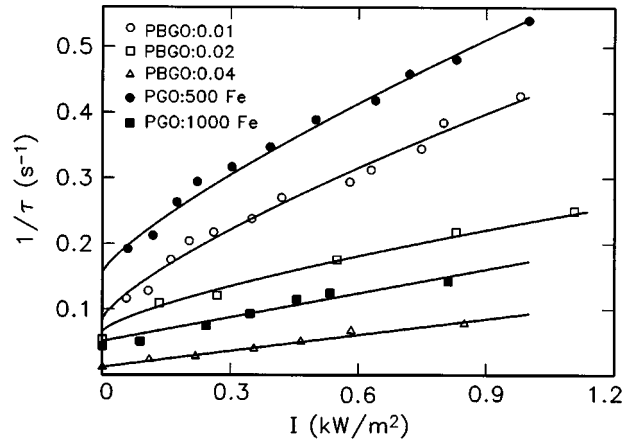


FIG. 6. Inverse decay time constant τ^{-1} as a function of erase beam intensity I at room temperature for different samples. The symbols are measured data, and the lines are fittings according to $\tau^{-1} = (\sigma_d + \sigma_p) / \epsilon \epsilon_0$. The values of photoconductivity at an intensity of $I = 3 \text{ kW/m}^2$ are listed in Table II.

toconductivity as is the case in other photorefractive crystals.^{15,18} Rh doping, however, leads to hardly any observable changes in conductivity. For the intensity range below 1 kW/m^2 used in this measurement, photoconductivity depends sublinearly on light intensity ($x < 1$ as listed in Table II). For the samples with 1000 ppm Fe or with Ba ($x = 0.04$), the photoconductivity depends almost linearly on light intensity. The measured results for undoped and Rh-doped samples are not included in Fig. 6, because their inverse decay time constants are more than one order of magnitude larger than those of the other samples.

The dependence of photoconductivity on light intensity is determined also by measuring the diffraction efficiency as a function of writing beam intensity. The fitting to the experimental results by taking Eq. (7) into consideration gives the dependence of photoconductivity on light intensity. There is relatively good agreement with the results obtained with these two methods. For example, the value x determined by diffraction measurements is 0.75, which agrees fairly well with $x = 0.72$ obtained by the decay time measurements. Based on these results we calculated the photoconductivity for different samples at $I = 3 \text{ kW/m}^2$, which is the intensity of the writing beams in holographic recording. The results are given in Table II.

TABLE II. Measured parameters for different samples.

Sample	σ_d $10^{-11}(\Omega \text{ m})^{-1}$	σ_p (3 kW/m ²) $10^{-10}(\Omega \text{ m})^{-1}$	x ($\sigma_p \propto I^x$)	E_A (eV)	N_{eff} (10^{22} m^{-3})	$\xi(K)$ $K = 2.35 \mu\text{m}^{-1}$
PGO	50.2	11.2	0.72	0.61	1.16	0.31
PBGO:0.01	3.0	2.8	0.76	0.49	1.13	0.19
PBGO:0.02	2.3	1.4	0.72	0.46	0.82	0.15
PBGO:0.04	0.38	0.89	0.98	0.49
PGO:500 Fe	5.5	3.3	0.79	0.47	0.48	0.26
PGO:1000 Fe	1.9	1.5	0.99	0.81	1.08	0.25
PGO:500 Rh	50.2	17.1	0.73	0.47	0.89	0.22

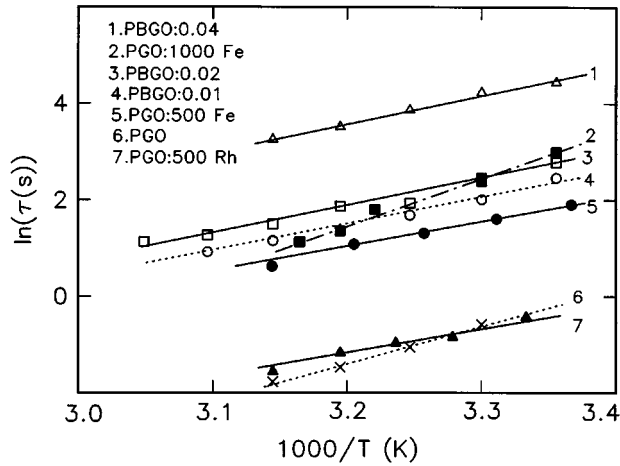


FIG. 7. Inverse dark decay time constant τ_d^{-1} as a function of inverse temperature T^{-1} for different samples. The symbols are measured data, and the lines are fittings according to $\tau_d = \tau_0 \exp(E_A/k_B T)$ where E_A is the activation energy listed in Table II.

3. Activation energy

After recording the holographic grating, we turned off both writing beams and probed the diffraction efficiency with a weak red He-Ne beam ($I < 0.01$ kW/m²). The decay of the grating can be considered as dark decay and the inverse dark decay time constant τ_d is measured as a function of temperature as presented in Fig. 7. The fitting to the experimental data using Eq. (11) gives the activation energy E_A for the different samples. As listed in Table II, the activation energy for the undoped sample is 0.61 eV, and doping decreases it to values less than 0.5 eV with the exception of the heavily Fe-doped sample in which E_A becomes larger than that for the undoped sample.

4. Electron-hole competition

In a two-wave mixing experiment we have measured the exponential gain in different samples with the same grating spatial frequency $K = 2.35 \mu\text{m}^{-1}$. Using the effective charge density obtained, and the photo- and dark conductivity listed in Table II, we can deduce the electron-hole competition factor $\xi(K)$ following Eqs. (13)–(15). The results are presented also in Table II.

In the above calculation the electrooptic coefficients for all the samples are supposed to be the same. This might introduce some errors, especially for the samples that contain Ba. As mentioned in section I the crystals containing Ba have a lower Curie temperature which may enlarge the elements of the electrooptic tensor slightly. In addition we have measured the dielectric constant ϵ_{33} for samples PBGO:0.01 and PBGO:0.02, whose values are 42 and 46 at room temperature, respectively. They have been considered in our calculation. From the results listed in Table II, we see that doping decreases the electron-hole competition factor.

V. DISCUSSION

The maximum refractive index modulation Δn_{max} of a photorefractive grating is related to the diffusion field E_D ,

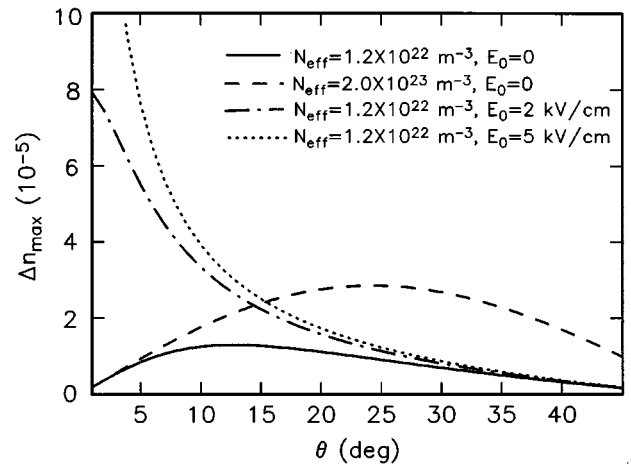


FIG. 8. Calculated maximum refractive index modulation Δn_{max} of a holographic grating as a function of the half-crossing angle θ between two interacting beams inside the crystal for different values of the effective charge density N_{eff} and external electric field E_0 . The factor C (see Eq. (5)) is supposed to be 1, and the two beams with the same intensity are incident symmetrically ($\beta=0$) to the crystal.

which depends on the grating spatial frequency, the applied electric field E_0 , the limiting space-charge field E_Q , and the polarization of the interacting beams as described in section III. The calculated values of Δn_{max} are shown in Fig. 8 as a function of the half beam angle θ between the writing beams inside the crystal for different values of E_0 and different effective charge densities N_{eff} . In this calculation the factor C in Eq. (5) is supposed to be 1 and the two extraordinarily polarized beams are symmetrically incident to the crystal. Applying an electric field can lead to a substantial increase of the refractive index modulation. Indeed, Δn in the undoped sample has been increased by more than one order of magnitude when we apply an external electric field $E_0 = 10$ kV/cm compared to the case $E_0 = 0$.

The increase of the effective charge density by doping is a usual way to improve the photorefractive effect in other materials,¹⁹ but in the present work we have not found any evidence that the effective charge density is increased in the doped samples. The photorefractive effect in this material may be caused by intrinsic defects. Nevertheless, holographic measurements show that some parameters such as conductivity, activation energy level, etc. are really changed by doping. Perhaps other dopants and/or further annealing may influence the photorefractive effect in this material.

It should be noted that in contrast to our work, Królikowsky *et al.*⁶ deduced negative charges to be responsible for the buildup of the fast grating. In their paper they did not mention the growth atmosphere, but during the poling a coloration of the crystal is observed and the results are restricted to this colored sample. In our work this process is avoided by using a much smaller electric field during poling. This difference might be the reason for the different type of charges measured in our experiments.

A further question is why we can attribute the measured smaller effect to electron-hole competition. To clarify this, we analyze the measured exponential gain for the slow and

the fast gratings in section IV A. For the slow grating, even if we do not consider the limiting space-charge field (which can limit the space-charge field at large grating spatial frequency), the measured gain can be predicted approximately by the theoretical calculation. But in the case of the fast grating, the measured gain is always much smaller than the calculated one. The experimental conditions are exactly the same for both measurements, and the influence of dark- and photoconductivity has been considered. Thus the only possible explanation is the consideration of electron-hole competition by the one-center model.¹¹

In conclusion, different kinds of gratings are observed in lead germanate crystals; among them the fast grating is determined to originate from the electrooptic photorefractive effect. Basic properties concerning the fast grating in both undoped and doped samples are studied and electron-hole competition is found to be the main factor to limit the space-charge field. Intrinsic defects seems to play an important role. Additional doping with Fe, Rh or the adding of Ba can change some parameters but it does not enhance the photorefractive effect significantly in this material.

ACKNOWLEDGMENTS

The authors thank Professor E. Krätzig for the valuable discussion and suggestion. Financial support of the Deutsche Forschungsgemeinschaft (SFB 225) and of the Friedrich-Ebert-Stiftung are gratefully acknowledged.

- ¹*Photorefractive Materials and Their Application II*, Topics in Applied Physics, Vol. 62 (Springer, Berlin, 1989).
- ²K. Buse, *Appl. Phys. B: Lasers Opt.* **64**, 391 (1997).
- ³F. Kahmman, J. Badura, R. B. K. Lytze, and R. A. Rupp, *Appl. Phys. A: Solids Surf.* **57**, 77 (1993).
- ⁴H. Iwasaki, K. Sugii, and S. Miyazama, *Mater. Res. Bull.* **6**, 503 (1971).
- ⁵*Landolt Börnstein—Numerical Data and Functional Relationships in Science and Technology, New Series, III/16*, edited by K.-H. Hellwig (Springer, Berlin, 1981).
- ⁶W. Królikowski, M. Cronin-Golomb, and B. S. Chen, *Appl. Phys. Lett.* **57**, 7 (1990).
- ⁷M. Simon, F. Mersch, C. Kuper, S. Mendricks, S. Wevering, J. Imbrock, and E. Krätzig, *Phys. Status Solidi A* **159**, 559 (1997).
- ⁸X. Yue, J. Xu, F. Mersch, R. Rupp, and E. Krätzig, *Phys. Rev. B* **55**, 9495 (1997).
- ⁹H. Kogelnik, *Bell Syst. Tech. J.* **48**, 2909 (1969).
- ¹⁰N. V. Kukhtarev, V. B. Markov, S. Odoulov, M. S. Soskin, and V. L. Vinetskii, *Ferroelectrics* **22**, 949 (1979).
- ¹¹M. C. Bashaw, T.-P. Ma, and R. C. Barker, *J. Opt. Soc. Am. B* **9**, 1666 (1992).
- ¹²J. P. Herriau, D. Rojas, J. P. Huignard, J. M. Bassat, and J. C. Launay, *Ferroelectrics* **75**, 271 (1987).
- ¹³A. Grunnet-Jepsen, I. Aubrecht, and L. Solymar, *J. Opt. Soc. Am. B* **12**, 921 (1995).
- ¹⁴K. Buse, *Appl. Phys. B: Lasers Opt.* **64**, 273 (1997).
- ¹⁵M. D. Ewbank, R. R. Neurgaonkar, W. K. Cory, and J. Feinberg, *J. Appl. Phys.* **62**, 374 (1987).
- ¹⁶E. Guibelalde, *Opt. Quantum Electron.* **16**, 173 (1984).
- ¹⁷D. L. Staebler, in *Holographic Recording Materials*, Topics in Applied Physics, Vol. 20, edited by H. M. Smith (Springer, Berlin, 1977).
- ¹⁸R. A. Vazquez, R. R. Neurgaonkar, and M. D. Ewbank, *J. Opt. Soc. Am. B* **9**, 1416 (1992).
- ¹⁹P. Günter, *Phys. Rep.* **93**, 199 (1982).